E-Article

Trait-Based Modeling of Multihost Pathogen Transmission: Plant-Pollinator Networks

Lauren L. Truitt,[1,*] Scott H. McArt,[1] Andrew H. Vaughn,[2] and Stephen P. Ellner[2,†]

1. Department of Entomology, Cornell University, Ithaca, New York 14853; 2. Department of Ecology and Evolutionary Biology, Cornell University, Ithaca, New York 14853

Submitted May 14, 2018; Accepted December 18, 2018; Electronically published April 29, 2019

Online enhancements: appendix. *Dryad data:* https://dx.doi.org/10.5061/dryad.730n045.

ABSTRACT: Epidemiological models for multihost pathogen systems often classify individuals taxonomically and use species-specific parameter values, but in species-rich communities that approach may require intractably many parameters. Trait-based epidemiological models offer a potential solution but have not accounted for within-species trait variation or between-species trait overlap. Here we propose and study trait-based models with host and vector communities represented as trait distributions without regard to species identity. To illustrate this approach, we develop susceptible-infectious-susceptible models for disease spread in plant-pollinator networks with continuous trait distributions. We model trait-dependent contact rates in two common scenarios: nested networks and specialized plant-pollinator interactions based on trait matching. We find that disease spread in plant-pollinator networks is impacted the most by selective pollinators, universally attractive flowers, and cospecialized plant-pollinator pairs. When extreme pollinator traits are rare, pollinators with common traits are most important for disease spread, whereas when extreme flower traits are rare, flowers with uncommon traits impact disease spread the most. Greater nestedness and specialization both typically promote disease persistence. Given recent pollinator declines caused in part by pathogens, we discuss how trait-based models could inform conservation strategies for wild and managed pollinators. Furthermore, while we have applied our model to pollinators and pathogens, its framework is general and can be transferred to any kind of species interactions in any community.

Keywords: infectious disease, model, nestedness, plant-pollinator network, specialization, trait.

Introduction

Community ecologists have begun to make great strides in understanding multispecies interactions through trait-based approaches, identifying key functional attributes of organisms (size, shape, nutrient requirements, etc.) that are important for community structure and function (e.g., Hillebrand and Matthiessen 2009; Allison 2012; Urban-Mead 2017). Consequently, there is a surge of interest in exploring how an explicit consideration of traits can improve understanding of multihost pathogen transmission (Paull et al. 2012; Rudge et al. 2013; Streicker et al. 2013; Stutz et al. 2014; Han et al. 2015; Luis et al. 2015). At the same time, disease spread models are often improved when species interaction networks are considered (Otterstatter and Thomson 2007; Salathe et al. 2010; White et al. 2017). However, the merging of trait-based approaches with network modeling to understand multihost transmission across space and time is in its infancy. Most studies investigating the importance of traits have limited or no knowledge of contact patterns among hosts (e.g., Rudge et al. 2013; Han et al. 2015; Luis et al. 2015). Furthermore, to our knowledge, no theory has been developed to understand how traits may predict multihost pathogen transmission in networks of interacting species.

A trait-based approach to modeling disease dynamics may be advantageous for several reasons. First, a trait-based approach can consider within-species variation, which can be an important source of heterogeneity in disease transmission, affecting susceptibility, contact rates with other hosts, duration of infectiousness, and pathogen shedding rates (Perkins et al. 2003; Lloyd-Smith et al. 2008; Hudson et al. 2008; Hawley and Altizer 2011; Strauss et al. 2018). Second, results have the potential for across-community generality, due to taxon independence and because traits can be linked to the environment (e.g., Rudge et al. 2013). Thus, predictions across multiple environmental contexts are facilitated (McGill et al. 2006; Green et al. 2008; Webb et al. 2010; Strauss et al. 2018). Finally, a trait-based approach can drastically simplify data analysis and modeling by reducing the number of parameters needed (Dobson 2004). Relationships between measurable traits and model parameters can be estimated for

* Present address: National Heart, Lung, and Blood Institute, Bethesda, Maryland 20814.

† Corresponding author; email: spe2@cornell.edu.

ORCIDs: Vaughn, https://orcid.org/0000-0003-3113-2981; Ellner, https://orcid.org/0000-0002-8351-9734.

Am. Nat. 2019. Vol. 193, pp. E149–E167.
DOI: 10.1086/702959

a subset of species spanning the range of candidate traits, and epidemiological parameters for other species can then be imputed.

Here we use plant-pollinator networks to advance trait-based modeling of multihost pathogen transmission. A growing number of studies show that many pathogens are shared between bee species (Goulson 2009; Cornman et al. 2012; Evison et al. 2012; Ravoet et al. 2014; Gamboa et al. 2015; McMahon et al. 2015). Furthermore, a broad literature exists regarding the structure and function of plant-pollinator networks (e.g., Bascompte et al. 2003; Memmott et al. 2004; Lever et al. 2014). These studies consistently show that nestedness and specialization in plant-pollinator networks are common (Bascompte et al. 2003; Aizen et al. 2012; Burkle et al. 2013), resulting in heterogeneity among potential hosts in contact patterns at flowers. Thus, there is great opportunity for host community composition (Ruiz-Gonzalez et al. 2012) and network architecture to alter pathogen transmission dynamics. Although more than 50 studies have documented the importance of traits such as nectar volume, stigma length, and bee foraging duration for transmission of plant pathogens at flowers, how bee and flower traits affect transmission of pollinator pathogens is almost completely unexplored (McArt et al. 2014; Koch et al. 2017; but see Adler et al. 2018). Considering that global pollinator declines are caused in part by pathogens (Cameron et al. 2011; Goulson et al. 2015), further understanding of how traits impact disease transmission among pollinators is needed.

To develop our model, we use community-wide functions in which model parameters are functions of individual-level traits. We first propose a simple single-class model (analogous to a single-species model) for pollinator-flower pathogen transmission. We then consider pathogen transmission in a community of multiple bees and flowers characterized by trait values that vary continuously within and across species, rather than positing a discrete set of species where individuals within a species are identical in traits and therefore in parameter values. The difference between these two perspectives is illustrated by the two representations in figure 1 of the distribution of corolla tube length, a flower trait that affects foraging preferences and efficiency by different-size pollinators (e.g., Harder 1983; Miller-Struttmann et al. 2015). While some species (such as *Alliara*) could be characterized by a single value, many have wide and broadly overlapping distributions. If epidemiological parameters really are primarily trait dependent (with species identity less important), the distribution of trait values without regard to species identity may be the most effective way to characterize a multispecies community.

To illustrate our proposed approach based on trait distributions, we construct and study a model in which traits define the pattern of visitation within the community. We analyze the model to identify which locations in the network are most important for disease persistence (i.e., for making the pathogen reproduction number $R_0 > 1$) and for steady-state disease prevalence in pollinators and to identify which processes and parameters are most important. This is done through sensitivity analysis of R_0 and steady-state disease prevalence, with respect to perturbations of parameters or class abundances. We compare the results for two types of interactions—nested interaction networks (Bascompte and Jordano 2007) and specialized interactions based on plant-pollinator trait matching—and for uniform versus nonuniform trait distributions. In pollination networks, nestedness refers to visitation patterns where all pollinators visit certain flowers with universally attractive characteristics, while a smaller subset of pollinators also visit flowers that are less universally attractive. Specialization refers to visitation patterns in which contact rates are greatest between bees and flowers with specific alignments of traits. Finally, because we are interested in how traits and relative abundance jointly impact disease dynamics, we modeled communities with both uniform and nonuniform trait distributions. Computer scripts to replicate our figures and results have been deposited in the Dryad Digital Repository (http://dx.doi.org/10.5061/dryad.730n045; Truitt et al. 2019).

Models

In all our models, a "class" refers to a group of individuals with identical values of all parameters that affect their demography and disease transmission. To introduce our assumptions, we first present a model with one class each of bees and flowers. We then develop the continuous trait distribution (CTD) model, where a class is defined by the specific value of a quantitative trait that can take any value in an interval. For numerical solutions, the CTD model is approximated by a discrete multiclass model where individuals are binned into small subintervals and assigned the bin midpoint as their trait value.

Single-Class Model

The model is intended to balance simplicity and biological relevance. Figure 2*A*, 2*B* represents the model pictorially. Individual bees and flowers are categorized as either susceptible, S_B and S_F, or infected with the focal pathogen, I_B and I_F, without any latent period. The total population sizes are thus $N_B = S_B + I_B$ for bees and $N_F = S_F + I_F$ for flowers. An infected flower might be more accurately described as a contaminated flower, as we assume that pathogen presence has no direct effect on the flower. All uninfected bees are susceptible to pathogen transmission, and all infected bees are equally infectious; for simplicity, we assume the same for flowers. Homogeneity of bee susceptibility also

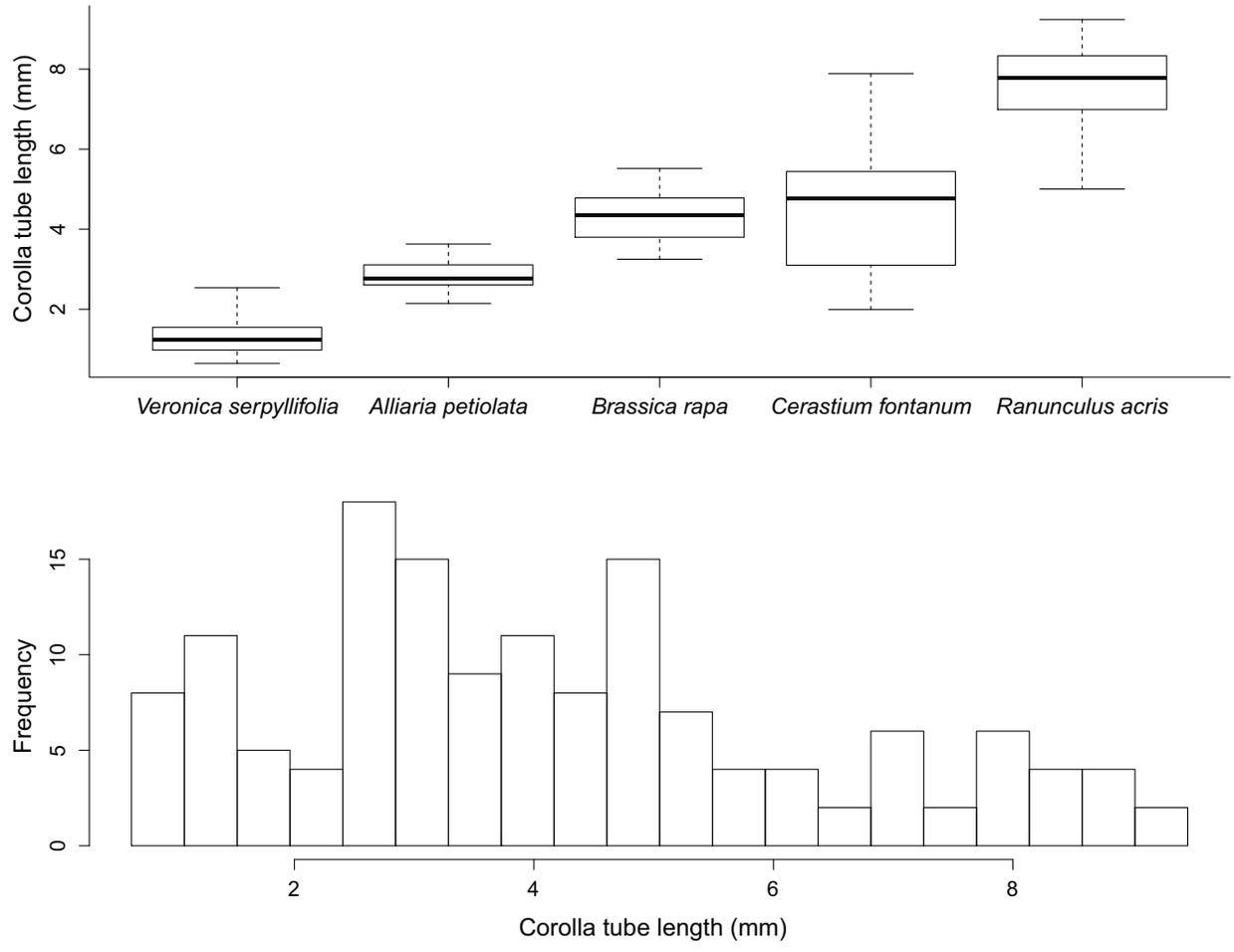

Figure 1: Distribution of corolla tube length for five common flowering plant species in three old-field communities in upstate New York in 2017. *Top*, boxplots for each species. Boxes extend from the 25th to 75th percentiles, and whiskers extend to the 5th and 95th percentiles. *Bottom*, histogram of pooled values from all five species. This figure was produced by PlotTraitDistributions.R (computer scripts deposited in the Dryad Digital Repository: https://dx.doi.org/10.5061/dryad.730n045; Truitt et al. 2019).

may not be completely realistic (Retschnig et al. 2014), and we are not aware of any evidence bearing on homogeneity of bee infectiousness. However, these are beyond the scope of this article.

N_F is assumed to be constant on the time scale of the model (no births or deaths), while bee population size changes with constant birthrate b and constant per capita death rates for susceptible bees, μ_S, and infected bees, μ_I (Michener 1974; Winston 1987; Barrett and Harder 2007; Goulson 2009). Flowers remain infected for very brief periods at our baseline parameter values (0.5 day; table 1), and at any given moment most flowers are uninfected. Allowing flowers in the model to die and be replaced by new, uninfected flowers would therefore have little effect on disease outcomes.

Bees and flowers each have constant rates of recovery from infection, γ and ζ, respectively. We assume that bees and flowers return to being susceptible on recovery, with the same susceptibility to a repeat infection as all other susceptibles. In bees, recovery is mediated by the host immune response (Evans et al. 2006). In flowers, the time to recovery is determined by the pathogen's ability to survive in the environment, involving factors such as solar radiation and desiccation that vary among pathogens and environments. Pathogen viability outside its host significantly impacts transmission dynamics (Merikanto et al. 2012).

Finally, we assume that there is no direct bee-to-bee or flower-to-flower transmission. Intracolony transmission occurs in social bees (Naug 2008), but here we only consider foraging bees where pathogens are transmitted in the environment via infected flowers (i.e., transmission in plant-pollinator networks).

To complete the model, we need to specify the rates of infection, which depend on the rates at which susceptible bees visit infected flowers and infected bees visit susceptible

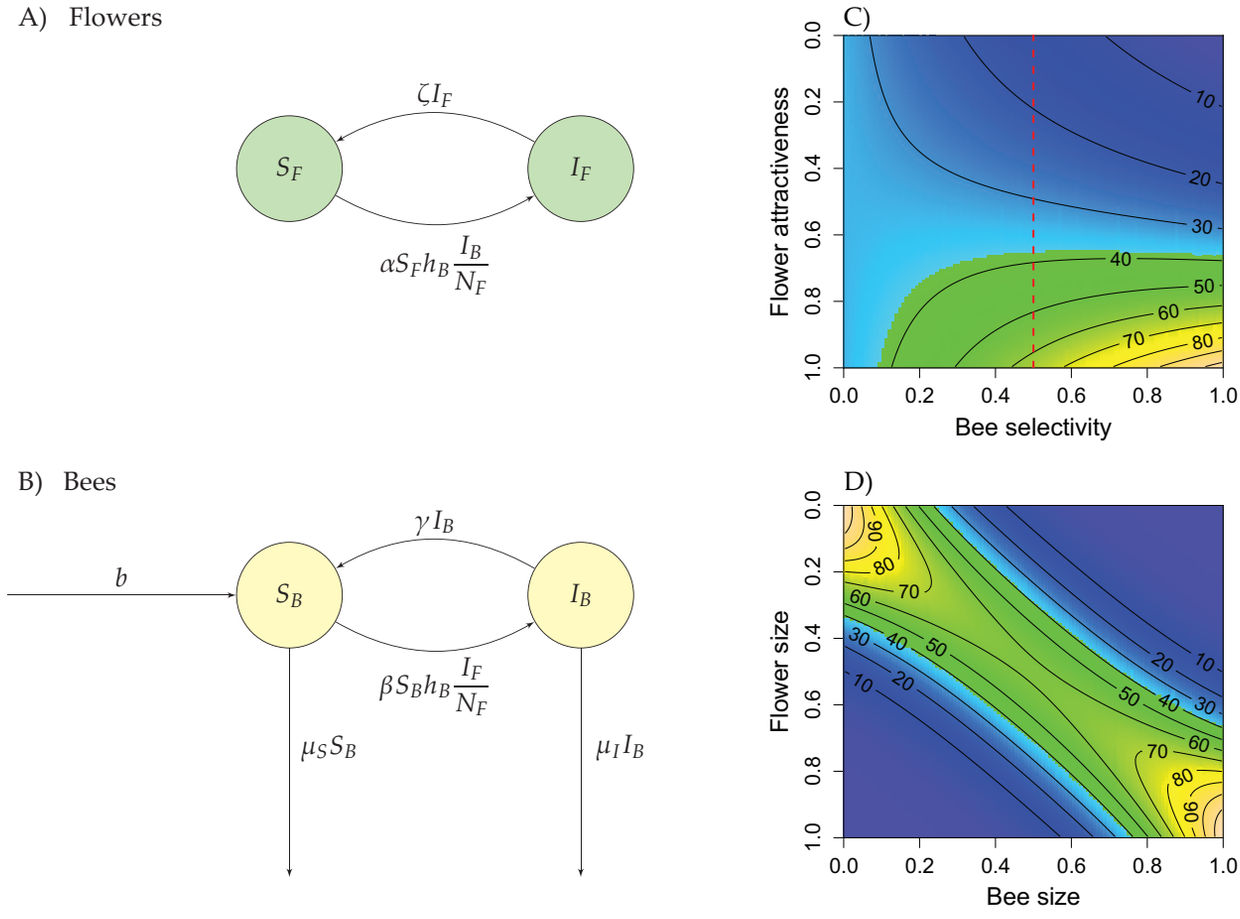

Figure 2: Summary of the model. *A*, *B*, Compartment diagram for the one-class susceptible-infectious-susceptible (SIS) model for flowers and bees, respectively. *C*, *D*, Continuous trait distribution model: image and contour plots of contact rates in the continuous trait distribution nestedness ($n = 3$) and specialization ($\sigma = 10$) models, respectively. Warmer colors (yellows) indicate a greater frequency of visitation when compared to cooler colors (blues). A vertical slice (such as the dashed red vertical line in *C*) represents the preferences of one bee class. In the nestedness model, all bees prefer more attractive flowers, but more selective bees have a stronger preference. In the specialization model, bees prefer flowers whose size (scaled corolla length) matches their size (scaled tongue length). Midsize bees can visit flowers larger or smaller than themselves, but extreme-size bees can only visit less extreme flowers and so are more concentrated on those. Panels *C* and *D* were produced by NetworkImages.R (computer scripts deposited in the Dryad Digital Repository: https://10.5061/dryad.730n045; Truitt et al. 2019).

flowers. We assume that bees visit flowers without regard to their state of infection. Let h_B denote the flower visitation rate by an individual bee, susceptible or infected (flowers/bee/day), and α the probability of bee-to-flower transmission when an infected bee visits an uninfected flower. Infected bees visit flowers at total rate $h_B I_B$, so each susceptible flower is visited at rate $h_B I_B / N_F$ and infected with probability α on each visit. The rate of new flower infections is therefore $\alpha S_F h_B I_B / N_F = \alpha(N_F - I_F) h_B I_B / N_F$.

Similarly, let β be the probability of flower-to-bee pathogen transmission when a susceptible bee visits an infected flower. Each susceptible bee has infectious contacts at rate $h_B I_F / N_F$, so new bee infections occur at total rate $\beta S_B h_B I_F / N_F$. We therefore have the following differential equations for susceptible and infected bees and infected flowers:

$$\frac{dS_B}{dt} = b + \gamma I_B - \beta S_B h_B \frac{I_F}{N_F} - \mu_S S_B, \tag{1a}$$

$$\frac{dI_B}{dt} = \beta S_B h_B \frac{I_F}{N_F} - (\mu_I + \gamma) I_B, \tag{1b}$$

$$\frac{dI_F}{dt} = \alpha(N_F - I_F) h_B \frac{I_B}{N_F} - \zeta I_F. \tag{1c}$$

R_0 *for the Single-Class Model.* Now we will consider the reproduction number, R_0, defined as the number of secondary

Table 1: Assumed (default) values of model parameters used for local sensitivity analysis and the ranges of values used for global sensitivity analysis

Parameter	Definition	Units	Value (Range)	Reference
N_F	Total flower population	Flowers or inflorescences	2,204,970 (988,163–4,827,353)	A. Iverson, unpublished data
N_B^*	Total bee population	Individuals	285 (190–380)	Mandelik et al. 2012
$(I_B/N_B)^*$	Infection prevalence in bees	Proportion	.21 (.06–.32)	Figueroa et al., forthcoming *b*
b	Total birthrate of bees	Bees/day	9.1 (6.1–12.3)	Set to match default N_B
μ_S	Death rate of susceptible bees	Day^{-1}	.032 (.02–.077)	Michener 1974, 2007; Winston 1987; Goulson 2009
μ_I	Death rate of infected bees	Day^{-1}	.051 (.032–.123)	Paxton et al. 2007; Graystock et al. 2013*a*, 2013*b*; Furst et al. 2014; McMahon et al. 2016
h_B	Contact rate of one bee with all flowers	Visits/bee/day	4,032 (1,632–6,432)	Couvillon et al. 2015
α	Probability of transmission from infected bee to noncontaminated flower	Proportion	.014 (.003–.07);	Figueroa et al., forthcoming *a*
β	Probability of transmission from contaminated flower to susceptible bee	Proportion	Adjusted	Adjusted for each network, to match R_0 estimated from default I_B/N_B
γ	Bee rate of recovery from infection	Day^{-1}	.10 (.05–24)	Winston 1987
ζ	Flower rate of recovery from infection	Day^{-1}	2 (1–48)	Figueroa et al., forthcoming *a*; Kaya 1977

Note: Parameter values such as numbers of flowers and bees refer to a circular area of 100 m radius, which is a typical foraging radius of many species of wild bees (Zurbuchen et al. 2010). Items marked with an asterisk are state variables not parameters but are included here because N_B is used to estimate b, and observed infection prevalence in bees I_B/N_B is the basis for estimating R_0. The "reference" column states the main source of empirical information. Detailed justifications for default values and ranges are in the section on parameter values. Honeybees have extreme outlier values for some parameters, and the parameter ranges do not include honeybees in those cases.

infectious cases resulting from a single initial infection in an otherwise completely susceptible population (MacDonald 1952; Smith et al. 2012). Reproduction number R_0 is a useful characterization because a disease spreads if the number of infected individuals increases from an initially low level, generally when $R_0 > 1$.

Because there are two directions of transmission, we define two reproductive numbers. Let $T_{F,B}$ be the reproduction number for bee-to-flower transmission and $P_{B,F}$ the reproduction number for flower-to-bee transmission. Generally, the reproduction number is calculated as the product of the mean duration of infection, with the rate of secondary infections caused by one infected individual when all others are susceptible. For bee-to-flower transmission,

$$T_{F,B} = \frac{\alpha h_B}{\gamma + \mu_I} \tag{2}$$

because an infected bee remains infected for $(\gamma + \mu_I)^{-1}$ time units, on average, and contaminates $h_B\alpha$ flowers per unit time in a completely susceptible flower population. Similarly, for flower-to-bee transmission,

$$P_{B,F} = \frac{\beta \bar{N}_B h_B}{N_F \zeta}. \tag{3}$$

Here $\bar{N}_B = b/\mu_S$ is the steady-state bee population when the population is disease free, so $\bar{N}_B h_B/N_F$ is the rate of bee visits to any one flower. A flower spends ζ^{-1} time units contaminated and infects $\beta\bar{N}_B h_B/N_F$ bees per unit time, in a completely susceptible bee population.

Consequently, the bee-to-bee (and flower-to-flower) reproduction number is

$$R_0 = P_{B,F}T_{F,B} = \frac{\alpha\beta\bar{N}_B h_B^2}{N_F\zeta(\gamma + \mu_I)}. \tag{4}$$

In some models, a disease can persist even when $R_0 < 1$ (Li et al. 2011). Consequently, we ran simulations of our single-class model to verify that the disease dies out when $R_0 < 1$ (script New Simulations.R). A thousand simulations for each

condition ($R_0 < 1$, $R_0 > 1$) were run by drawing parameters other than β from independent uniform distributions on the "global" parameter ranges (table 1; discussed below) and then drawing β so that the R_0 was uniformly distributed between 0.05 and 0.98 (for $R_0 < 1$) or uniformly distributed between 1.05 and 10 (for $R_0 > 1$). In 100% of these simulations, when $R_0 < 1$, the disease dies out, and when $R_0 > 1$, the disease persists. Figure S1 (figs. S1–S11 are available online) shows an example.

Continuous Trait Distribution Model

The usual way of extending our single-class model (and similar models) to a community of multiple pollinators and flowers would be a multispecies model in which each species is characterized by parameter values that are the same for all individuals in the species. This would produce a system of ordinary differential equations, with two equations (susceptible and infected) for each pollinator and flower species, with parameters including matrices characterizing all pairwise contact and disease-transmission rates. However, if parameters affecting pathogen transmission are primarily determined by individual traits, with species identity of secondary importance, we can instead view the bee and flower communities as a collection of individuals characterized by the frequency distribution of the relevant traits.

To introduce this approach, we specifically assume that bees and flowers in the community are both characterized by a measure of size (e.g., bee tongue length and flower corolla length), denoted x and y for bees and flowers, respectively, and scaled so that they range between 0 and 1. One style of trait-based model (e.g., Dobson 2004) assigns a particular size to each bee species and flower species, and the parameter values for each species are functions of its size; species are distinct, but individuals within a species are assumed to be homogeneous.

Here we propose an alternative in which traits (and, therefore, model parameters) are assumed to vary continuously among individuals, while species identity is ignored. We are not claiming that species identity is really irrelevant—bees use many species-specific flower attributes in their foraging decisions (see "Discussion"). However, we propose that the gains from a great reduction in parameter count may more than offset the loss of detail if a trait-centric model can capture the main features of cross-species interactions in a species-rich community.

The community is described by the trait-frequency distributions $N_B(x)$ and $N_F(y)$, such that $\int_{x_1}^{x_2} N_B(x)dx$ is the number of bees with trait values between x_1 and x_2, and similarly for $N_F(y)$. In some cases, N_B and N_F might have several modes corresponding to typical values for a few common species, but this is not necessarily the case (fig. 1). Here $\int_0^1 N_B(x)dx$ and $\int_0^1 N_F(y)dy$ are total bee and flower numbers, respectively, corresponding to the numbers N_B and N_F in the single-species model.

The model has state variables $S_B(x, t)$, $I_B(x, t)$, $S_F(y, t)$, and $I_F(y, t)$, where $\int_{x_1}^{x_2} S_B(x, t)dx$ is the number of susceptible bees with trait values in $[x_1, x_2]$ at time t, and similarly for the other state variables. Each bee and flower class ("class" now referring to a set of individuals with the same trait value) obeys the assumptions of the single-class model. To specify transmission rates, let $h(y, x)$ be the average rate of contacts one class-x bee has with all flowers of class y combined (to be precise, the average rate of contacts with all flowers of classes y to $y + dy$ is $h(y,x)dy + o(dy)$ for $dy \ll 1$). As in the single-class model, infection rates can be written in terms of $h(y, x)$ and trait-dependent transmission probabilities $\alpha(y, x)$ (bee to flower) and $\beta(x, y)$ (flower to bee). Contacts between susceptible class-x bees and infected class-y flowers occur at total rate $S_B(x, t)h(y, x)I_F(y, t)/N_F(y, t)$.[1] Contacts between infected class-x bees and susceptible class-y flowers occur at total rate $I_B(x, t)h(y, x)S_F(y, t)/N_F(y, t)$. We have $S_F(y, t) = N_F(y) - I_F(y, t)$, where $N_F(y)$ is constant over time by assumption.

Allowing the disease to be transmitted between bees and flowers of any class, we have (omitting for clarity the t argument in state variables)

$$\frac{\partial S_B(x)}{\partial t} = b(x) + \gamma(x)I_B(x) - S_B(x)\int_0^1 \left[h(y,x)\frac{I_F(y)}{N_F(y)}\beta(x,y)\right]dy - \mu_S(x)S_B(x), \tag{5a}$$

$$\frac{\partial I_B(x)}{\partial t} = S_B(x)\int_0^1 \left[h(y,x)\frac{I_F(y)}{N_F(y)}\beta(x,y)\right]dy - (\mu_I(x) + \gamma(x))I_B(x), \tag{5b}$$

$$\frac{\partial I_F(y)}{\partial t} = \left(\frac{N_F(y) - I_F(y)}{N_F(y)}\right)\int_0^1 h(y,x)I_B(x)\alpha(y,x)dx - \zeta(y)I_F(y). \tag{5c}$$

These equations can be generalized to higher-dimensional traits by modifying the integrals describing transmission to integrals over multivariate trait distributions. It is also possible to include trait dynamics (e.g., if individuals are born small and grow over time) by adding advection and/or diffusion terms to the right-hand sides, as in the McKendrick-von Foerster equations for size-structured populations, but that is beyond the scope of this article.

To solve the CTD model numerically, we used method of lines, a general approach in which partial differential equa-

1. As with $h(y, x)$, this is a convenient shorthand for a precise statement involving dx and dy.

tions are approximated by a system of ordinary differential equations. For a general description, see, for example, Griffiths (2016, sec. 3.8); for our model, method of lines works as follows: The bee and flower trait ranges $0 \le x, y \le 1$ are divided into Q and K even subintervals, respectively, with constant widths $\Delta x = 1/Q$ and $\Delta y = 1/K$. Each continuous trait distribution is represented by an evenly spaced set of mesh points at the subinterval midpoints,

$$\begin{aligned} x_q &= \frac{(q-0.5)}{Q}, \quad q = 1, 2, \cdots, Q; \\ y_k &= \frac{(k-0.5)}{K}, \quad k = 1, 2, \cdots, K. \end{aligned} \tag{6}$$

Equations (5) are then approximated by a system of differential equations for each state variable at each of the mesh points (i.e., $S_B(x_q)$, $I_B(x_q)$, $I_F(y_k)$), in which the integrals on the right-hand side are approximated using the values at the mesh points. For example, the differential equations for $S_B(x_q)$, $q = 1, 2, \cdots, Q$ are

$$\begin{aligned} \frac{dS_B(x_q)}{dt} &= b(x_q) + \gamma(x_q) I_B(x_q) \\ &\quad - S_B(x_q) K^{-1} \sum_{k=1}^{K} \left[h(y_k, x_q) \frac{I_F(y_k)}{N_F(y_k)} \beta(x_q, y_k) \right] \\ &\quad - \mu_S(x_q) S_B(x_q). \end{aligned} \tag{7}$$

We used the deSolve package (Soetaert et al. 2010) in R to solve these differential equations numerically. In section S.2 of the appendix (supplemental appendix, available online), we show that the method of lines solution to the CTD model (5) corresponds to a model with multiple discrete species (eq. [S7]) in which some "species"-specific parameters depend on the distances Δx and Δy between neighboring mesh points.

R_0 for the CTD Model. For the CTD model, R_0 is computed as the spectral radius of the bee-to-bee next-generation operator **G**, whose kernel G is given by the composition of the bee-to-flower and flower-to-bee next-generation kernels.

The bee-to-flower kernel T gives the trait distribution of flower infections resulting from a trait distribution of infected bees when infected bees are infinitesimally rare and flowers are all susceptible. We can calculate T as follows: A bee of trait x remains infected for expected time $1/(\gamma(x) + \mu_I(x))$. Flowers in $(y, y + dy)$ are contacted at total rate $h(y, x)dy$, with infection probability $\alpha(y, x)$. The expected number of infections in $(y, y + dy)$ is, therefore, $T(y, x)dy$, where

$$T(y, x) = \frac{h(y, x)\alpha(y, x)}{\gamma(x) + \mu_I(x)}. \tag{8}$$

The bee-to-flower next-generation operator is the map on the space of real-valued integrable functions f on $[0, 1]$,

$$f \to \int T(y, x) f(x) dx.$$

The flower-to-bee operator P can be derived very similarly. When there is a single infected flower with trait value y and otherwise all flowers and bees are uninfected (and, therefore, $I_B \equiv 0$, $S_B(x) = \bar{N}_B(x) = b(x)/\mu_S(x)$ on the right-hand side of eq. [5b]), $I_B(x)$ increases at rate $\bar{N}_B(x)h(y, x)\beta(x, y)/N_F(y)$. One such newly infected flower has this effect for expected time $1/\zeta(y)$, so we have

$$P(x, y) = \frac{\bar{N}_B(x)h(y, x)\beta(x, y)}{N_F(y)\zeta(y)} = \frac{b(x)h(y, x)\beta(x, y)}{\mu_S(x)N_F(y)\zeta(y)}. \tag{9}$$

The next-generation kernel G is the composition of P and T,

$$G(x^*, x) = \int P(x^*, y) T(y, x) dy. \tag{10}$$

The overall next-generation operator is the map

$$\mathbf{G} : i(x) \to \int G(x, u) i(u) du. \tag{11}$$

The reproductive number of the entire community is the dominant eigenvalue (spectral radius) of **G** (Diekmann et al. 2009; Yang 2014). To implement (10) and (11) numerically, we use midpoint-rule integration with the mesh points in equation (6), as is usually done with integral projection models (Ellner et al. 2016). Larger values of K and Q increase the accuracy of the approximation. This numerical approximation to the R_0 for the CTD model is equal to the R_0 for the corresponding discrete multiclass model (see sec. S.2.1).

As with the single-species model, we simulated the model to confirm that the disease dies out when $R_0 < 1$ and spreads when $R_0 > 1$, as in figure S2. One thousand simulations were again run for each condition, using the method of lines differential equations with $Q = K = 4$, drawing all parameters from their global ranges, and then scaling the matrix of β values by a constant to achieve uniform R_0 distributions on [0.05, 0.98] or [1.05, 10]. Again all simulations with $R_0 < 1$ led to the disease dying out, and all simulations with $R_0 > 1$ led to the disease persisting. The same was true for 1,000 simulations with narrower ranges of R_0 (0.9–0.98, 1.05–1.5).

Trait-Based Contact Rates

In general, bee and flower traits could affect attraction/preference, pathogen viability, or pathogen acquisition (e.g., McArt et al. 2014; Adler et al. 2018). Attraction and preference traits influence h, the rate of bee-flower contacts; viability-related traits will affect γ and ζ; and acquisition-related traits will influence α and β.

In this article, we focus on trait-determined contact rates. To do this, we assume that all other parameters are constant

across bee classes and across flower classes (including, for now, class abundance). We consider contact rates determined by a function $h(y, x)$ that specifies the average rate of contacts a bee with trait value x makes with flowers with trait value y. We will explore two types of contact network structure, specialization and nestedness, defined below.

As α, β, b, μ_S, μ_I, γ, N_F, and ζ are constant by assumption across bee and flower classes, it follows from equations (8) and (9) that the next-generation operator $\mathbf{G}$ is proportional to $\mathbf{H}^T\mathbf{H}$, where $\mathbf{H}$ is the operator with kernel $h(y, x)$ and $\mathbf{H}^T$ has kernel $h(x, y)$. Therefore, R_0 simplifies to

$$R_0 = \frac{\alpha\beta\bar{N}_B}{N_F\zeta(\mu_I + \gamma)}\lambda = \frac{\alpha\beta b}{N_F\zeta(\mu_I + \gamma)\mu_S}\lambda, \tag{12}$$

where λ is the spectral radius of $\mathbf{H}^T\mathbf{H}$. We evaluate λ numerically as the dominant eigenvalue of H^TH, where H is the $K \times Q$ matrix with entries $H_{k,q} = h_{k,q}$, the visitation rates in the approximating discrete multiclass model (eq. [S3]).

Nestedness. In pollination networks, nestedness refers to visitation patterns where all pollinators visit certain flowers with universally attractive characteristics, while a smaller subset of pollinators also visit flowers that are less universally attractive. Nestedness is common in plant-pollinator networks (Bascompte and Jordano 2007). For example, Miller-Struttmann et al. (2015) found that bumblebees with long tongues selectively visited flowers with long corolla tubes, while short-tongued bees were generalists with regard to corolla tube length. In that community, flowers with long corolla tubes are the most attractive, and long-tongued bees are more selective than short-tongued bees.

Now we propose a model for trait-dependent nestedness. Suppose that flowers have traits that impact their attractiveness to the bees in the community. Let $y \in [0, 1]$ be this level of attractiveness, where $y = 1$ is most attractive and $y = 0$ is least attractive. Additionally, we assume that bees are characterized by how selective they are in choosing which flowers to visit. Let $x \in [0, 1]$ be this level of selectivity, where $x = 0$ is least selective and $x = 1$ is most selective. We then assume that contact rates are given by

$$h(y, x) = C_x e^{-nx(1-y)}. \tag{13}$$

The parameter n determines the degree of nestedness; larger values of n correspond to greater nestedness. Further, C_x is the scalar value such that the total rate of contact for a class-x bee with all flower classes satisfies $\int_0^1 h(y, x)dy = h_B$. Thus, bee and flower trait values determine how bees divide their visits among different flower classes but do not affect the overall rate at which a bee visits flowers. Specifying the model this way lets us vary network structure (degree of nestedness) independent of the total rate of bee-flower contacts. This model is illustrated in figure 2*C*.

Specialization. Specialization refers to visitation patterns in which contact rates are highest between bees and flowers with specific alignments of traits. Our specialization model assumes that bees have a preferred flower trait, visiting flowers with this trait value and similar flowers most frequently and seldom visiting flowers with very different traits. In contrast to the nestedness framework, attractiveness is not universal: what one pollinator finds attractive, another does not. Bees often specialize in particular flowers according to several traits. For example, bees of the genus *Rediviva* with tarsi hairs of various length, which are used to collect oil, specialize in flowers of the genus *Diascia* by floral spurs (Michener 2007). While pollinator specialization on flowers is better studied, flower specialization on pollinators has also been shown (Betts et al. 2015).

To model specialization based on matching between bee and flower traits, let $x \in [0, 1]$ be the scaled bee trait and $y \in [0, 1]$ the scaled flower trait. We assume that contact rates are given by

$$h(y, x) = C_x e^{-\sigma(y-x)^2}, \tag{14}$$

where $\sigma \geq 0$ determines the degree of specialization in the network, where larger values of σ correspond to tightly specialized bees, and C_x is again the value that satisfies $\int_0^1 h(y, x)dy = h_B$. This network model is illustrated in figure 2*D*.

Parameter Values

Through an extensive literature review and use of our own data, we set default typical values and ranges of biologically relevant values for each parameter, given in table 1. As these values are used in all our subsequent analyses, their justifications are provided here, with some additional details in the "Further Explanations of Parameter Estimates" section of the appendix. Flower abundance and bee birthrate parameters are estimated for a circular area of 100 m radius, which is a typical foraging radius of many species of solitary wild bees (Zurbuchen et al. 2010) and would represent a region within which individuals are transmitting pathogens at shared floral resources. Our model's contact network represents the bees and flowers within this region, so bee birthrate refers to bees born within this region, and flower abundance refers to the number of flowers within this region. Honeybees and bumblebees have larger foraging radii (Visscher and Seeley 1982; Waddington et al. 1994; McArt et al. 2017), but our model is appropriate for many solitary bees, which are the largest fraction of bee abundance and diversity in the communities that we study empirically.

N_F: We used flower and inflorescence data from five eastern US old fields to estimate N_F (A. Iverson, unpublished data). We surveyed and identified all flowering plants in a

10 × 25-m plot in each field using the modified-Whittaker plot design (Stohlgren 2007; see app. B.1 for further details). These data allowed us to estimate flower or inflorescence density (as appropriate for each species) at daily time steps throughout the growing season. We estimated mean flower or inflorescence density for each species by calculating the mean daily density over the primary growing season (day of year 153–274, corresponding to June 1–Oct 1). All values were scaled up to represent flower/inflorescence density in a circle with a 100-m radius.

N_B: Based on Mandelik et al. (2012), we take 60–120 foraging bees per hectare as an estimate for bee abundance in old fields during the late spring and summer foraging seasons; this scales up to (rounding slightly) 190–380 foraging bees in a circle with a 100-m radius.

I_B/N_B: We used data from a study by Figueroa et al. (forthcoming *b*) that measured prevalence of three pathogens (trypanosomes, neogregarines, and *Nosema* spp.) among 586 bees representing 49 different species. The bees were obtained from wildflower plots near eastern US old fields. Pathogen prevalence in the bees was 32% for *Nosema*, 26% for trypanosomes, and 6% for neogregarines; we used the average of these as our default value.

b: We set values of b so that the steady-state bee abundance in the absence of disease (number in a circle of radius 100 m), which is b/μ_S, is in our range for N_B for the default value of μ_S.

μ_S: We estimate that the average life span of a foraging bee is 13 days to 7 weeks (Michener 1974; Winston 1987; Michener 2007; Goulson 2009). Assuming a constant adult mortality rate, the range of life spans translates to mortality rates of 0.02–0.077/day. The midpoint of the range of life spans is 31 days; our default value for μ_S is the inverse of the midpoint, 0.032/day.

μ_I: We assumed that infection with a pathogen reduces the bee's average life span by 37%, based on infection trials conducted across five pathogens (*Apicystis bombi*, *Crithidia bombi*, deformed wing virus, *Nosema apis*, and *Nosema ceranae*) in bumblebees and honeybees (Paxton et al. 2007; Graystock et al. 2013*a*, 2013*b*; Furst et al. 2014; McMahon et al. 2016).

h_B: Using flower visitation rate estimates from Couvillon et al. (2015) and an estimated foraging time of 8 h per day, we estimated that foraging bees visit between 1,632 and 6,432 flowers per day.

α: Figueroa et al. (forthcoming *a*) found that noninfected bumblebees defecate on 56% of flowers during a 3-h lab trial with 10–30 flowers, while *Crithidia*-infected bees defecated on 71% of flowers. We summarize these results by positing that bees defecate into 64% of 20 flowers within a 3-h period. If we assume that each defecation is into a randomly chosen flower, then a flower's probability of receiving none of N defecations is $(19/20)^N$. Solving $(19/20)^N = 0.36$ for N gives 20.5 defecations in a 3-h period. Then in an 8-h foraging period (visiting 4,032 flowers, in our model), it will defecate in a fraction $(20.5/3) \times 8/4{,}032 \approx 0.014$ of visited flowers. As this estimate is based on very limited data, we consider a wide range of possible values, fivefold up or down.

β: Because we were unable to find information that could be used to estimated β, we instead set β to give an R_0 value such that the infection prevalence in bees in the single-species model approximated the observed level of bee infection, I_B/N_B, as described above. We used the approximation $R_0 \approx (S/N)^{-1}$ (Keeling and Rohani 2008) to predict the range of β realistic values. In all of our analyses, we set all baseline parameter values except β to the values given in table 1 and then adjusted β such that $R_0 = 1.3$. These calculations are done in the provided R scripts for each analysis.

γ: At most, a pathogen can inhabit a bee for its entire lifetime. If a typical life span is 31 days (μ_S, above) and infection reduces this by 37%, we get 19.5 days as an upper bound on infection period. At the very least, a pathogen resides in the bee for a minimum of about 1 h before it is excreted in feces (Winston 1987). The midpoint of the range of infective periods is about 9.75 days; our default value of γ is the inverse of the midpoint, $\gamma = 0.10$. Combined with our estimate of μ_I, this says that roughly 2/3 of infected bees recover before dying of the disease.

ζ: Figueroa et al. (forthcoming *a*) estimated that bee pathogen *Crithidia bombi*, a protozoan, can live on flowers for at least 30 min, corresponding to $\zeta = 48$. For an upper limit, we used estimates from Kaya (1977) regarding viability of *Vairimorpha necatrix*, a plant pathogen that is closely related to *Nosema*, a common bee pathogen. On exposure to ultraviolet radiation mimicking sun exposure, Kaya (1977) showed that *V. necatrix* could survive at most 1 day on plants, corresponding to $\zeta = 1$. As our default, we therefore assumed a half-day mean infection period, so $\zeta = 2$.

Analyses

We used elasticity analyses to compare the importance of bees and flowers with different trait values and, therefore, with different positions in the trait-defined contact networks. Elasticity is defined as the fractional change in a response, relative to the fractional change in the perturbed parameter. The responses we considered were pathogen reproduction number R_0 (whose value determines whether the pathogen persists in the community) and pathogen prevalence in bees at steady state (i.e., the number of infected bees of all classes divided by the total number of bees). A parameter with positive elasticity causes the response variable to increase as the parameter value increases and vice versa for a parameter with negative elasticity. Magnitude (absolute value) of elasticity characterizes the impact of a particular parameter: if

parameter a has a larger magnitude of elasticity than parameter b, this means that a has a greater influence on the response variable. Two different types of comparison can be made. The first is comparing the same parameter (e.g., recovery rate) between bees with different trait values or between flowers with different trait values. A large response (and thus a high elasticity) when we perturb a parameter away from its trait-defined value for bees (or flowers) with a particular trait value shows that those bees play an especially important role in determining the response. The second is comparing different parameters for bees with the same trait value or flowers with the same trait value (e.g., recovery rate for bees with trait value 0.5 vs. death rate for the same bees). Doing this for all trait values in bees and flowers reveals which parameters are most important for determining the response.

We did elasticity analyses at two scales, local and global. Local elasticity analyses involve making small perturbations away from a trait-independent default value given in table 1 or away from the trait-dependent contact rate in the nested or specialized network model for bees or flowers of a particular trait value. This can be done using analytical sensitivity formulas, as explained in sections S.3 and S.4, or numerically by making small parameter changes and simulating the model to find the resulting change in the response. Global elasticity analyses involve varying simultaneously all parameters for trait values at all mesh points (eq. [6]) in bees and flowers across the entire range of biologically plausible values given in table 1. Multiple regression modeling of the response as a function of parameter values is then used to compare the relative impacts of different parameters. A detailed description of the global elasticity analyses methods is in the appendix ("Numerical Global Elasticity Analyses").

We considered three scenarios for trait distributions in the community. The first is a uniform trait distribution in both bees and flowers (achieved by making $N_F(y)$, $b(x)$, and $\mu(x)$ constant as functions of trait values). In the others, either bees or flowers have a nonuniform trait distribution where extreme trait values (x or y near 0 or 1) are less common than intermediate values, as shown in figure S6. This was done for bees by making $b(x)$ a nonconstant function of x with $\mu(x)$ trait independent and for flowers by making $N_F(y)$ nonconstant in y.

Results

In all cases (specialized or nested network and uniform or nonuniform trait distribution), local elasticity analysis shows that increasing b, α, and β have a positive effect on R_0, while increasing μ_S, μ_I, γ, ζ, and N_F have negative effects on R_0 (figs. 3–5). Most of these are intuitive: R_0 is increased by parameter changes that increase the number of bee-flower contacts, increase the chances of transmission per contact, or allow infected individuals to remain alive and infected for longer.

The negative effect of N_F (more flowers) is a dilution effect (Schmidt and Ostfeld 2001; Rudolf and Antonovics 2005). When more flowers of a given class are added, each one receives fewer visits (because bee foraging effort has not gone up in our model), and so each is less likely to become infected and thus less likely to infect a visiting bee.

Uniform Trait Distributions

We now explore the relative importance of bees and flowers with different traits. Consider first the case where traits are uniformly distributed across bees and flowers (i.e., N_F and b are the same for all flowers and bees, respectively). In the nested network model (fig. 3), R_0 is most sensitive to the parameters of the most attractive flowers and the most selective bees. In the specialization model, parameters of flowers and bees with intermediate traits (values near 0.5) impact R_0 more than those of flowers and bees with extreme traits (values near 0 or 1). Analytic sensitivity formulas (sec. S.3) confirm that the curves that visually appear to be exactly equal (b, α_B, and β_B; α_F and β_F; N_F and ζ) are indeed exactly equal in this case.

In both specialization and nestedness models, differences in elasticity among bee classes are relatively small, while differences among flower classes are considerably larger. In the asymptotic analyses for small n or σ (secs. S.6, S.7), the elasticities with respect to bee parameters are constant as a function of bee trait x (i.e., lines with zero slope and nonzero intercept), while the elasticities with respect to flower parameters are nonconstant. In the nested network, the flower trait elasticities are lines with nonzero slope, such that parameters of more attractive flowers have larger effects on R_0; in the specialization model, the flower trait elasticities are parabolas with maximum magnitude at the average flower trait $y = 0.5$.

For both scenarios, local elasticities are mirrored in a global sensitivity analysis (described in "Numerical Global Elasticity Analyses") over the entire range of parameter values given in table 1 (fig. S3) and in a local elasticity analysis of steady-state pathogen prevalence (fig. S4). All parameters have the same qualitative relationship between sensitivity and trait value and the same direction of effect on R_0, but the magnitudes differ among the three analyses. We also used global sensitivity analysis to determine how R_0 was affected by increased nestedness or specialization. We found $\partial R_0/\partial n$ was positive at 91% of parameter values in the nested network model, and $\partial R_0/\partial \sigma$ was positive at 85% of parameter values in the specialization model.

The patterns in contact rate elasticities also closely resemble the patterns in parameter elasticities (fig. 6), meaning that for both scenarios, the contacts that matter most

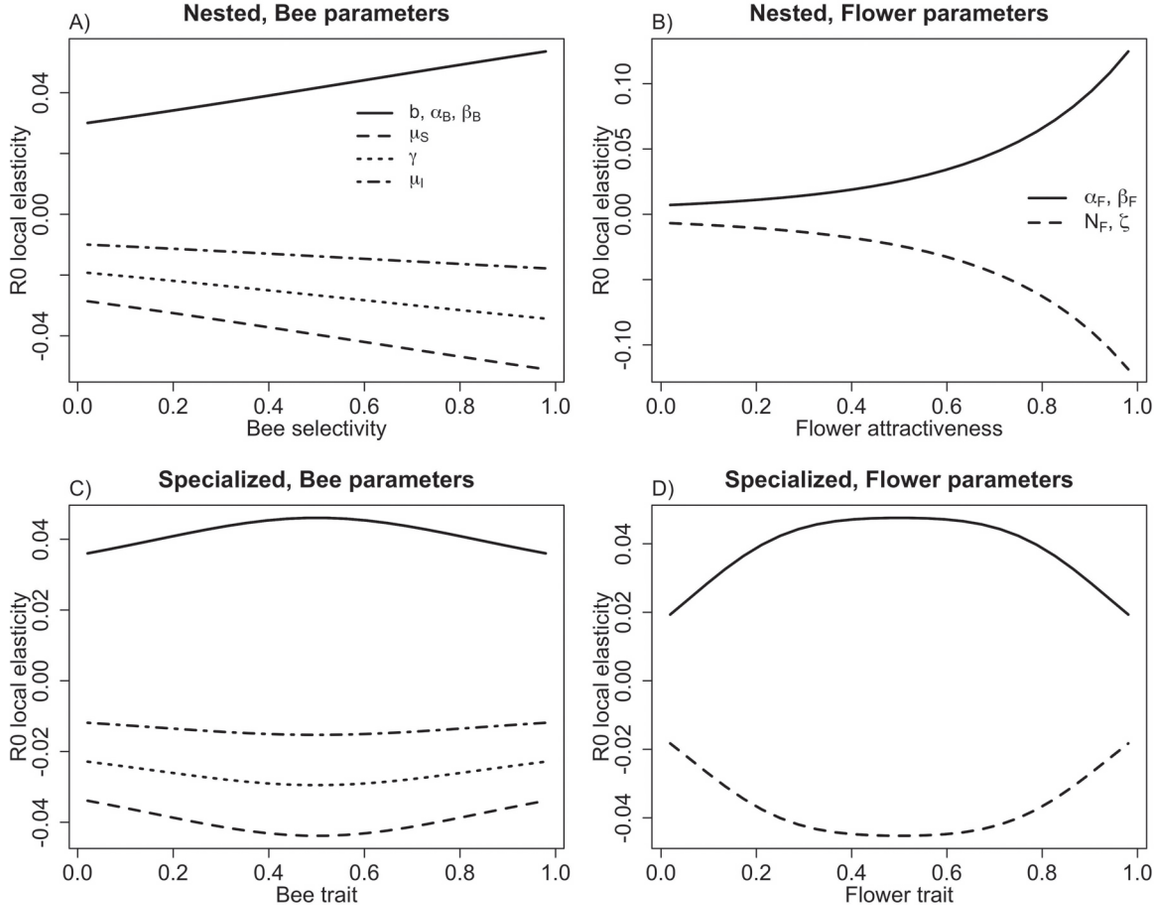

Figure 3: Local elasticity analysis of R_0 with respect to bee- and flower-specific parameters at the default parameter values. *A*, *B*, Bee- and flower-specific parameters in the nested network model. *C*, *D*, Bee- and flower-specific parameters in the specialized network model. Parameters in *C* and *D* are the same as in *A* and *B*, respectively: α_B, β_B refer to increasing by the same proportion all $\alpha(y, x)$ or $\beta(x, y)$ values, respectively, for a particular value of x; α_F, β_F refer to increasing all α or β values for a particular y. This figure was produced by R0_local_elasticity.R and scripts that it sources (computer scripts deposited in the Dryad Digital Repository: https://10.5061/dryad.730n045; Truitt et al. 2019).

are the contacts that happen most often. In the nested network model, the most important visits are between attractive flowers and selective bees. Importance decreases rapidly as flower attractiveness decreases and relatively slowly as bee selectiveness decreases. Figure 6*A* matches the perturbation analysis for weak nestedness (small n; sec. S.6). That analysis shows that for a flower of above-average attractiveness, increasing the transmission rate from a more selective bee has more effect on R_0 than increasing transmission from a less selective bee, while for a flower that is less attractive than average, increasing the transmission rate from less selective bees will have the larger effect on R_0. In the specialization model (fig. 6*B*), the most important contacts are near but not exactly on the diagonal line consisting of perfectly matched bee-flower pairs ($x = y$). Perturbation analysis for weak specialization (sec. S.7) shows that when σ is small, for any bee class x, the contact rate elasticity is maximized as a function of flower class y on the off-diagonal line $y = x/2 + 0.25$. In the limit $\sigma \to \infty$, the only contacts are between perfectly matched pairs, so elasticity is maximized on the diagonal $y = x$. The situation in figure 6*B* with $\sigma = 10$ is in between these limiting cases.

The importance of different bee and flower classes corresponds to disease prevalence at steady state, as seen in figure 7. As nestedness increases, disease prevalence for all classes increases; however, this is not the case in the specialization model, where greater specialization may mean that some bees or flowers are impacted more and some are impacted less.

Nonuniform Trait Distributions

Next, we consider the nonuniform trait distribution case (a scenario in which traits are distributed so that extreme

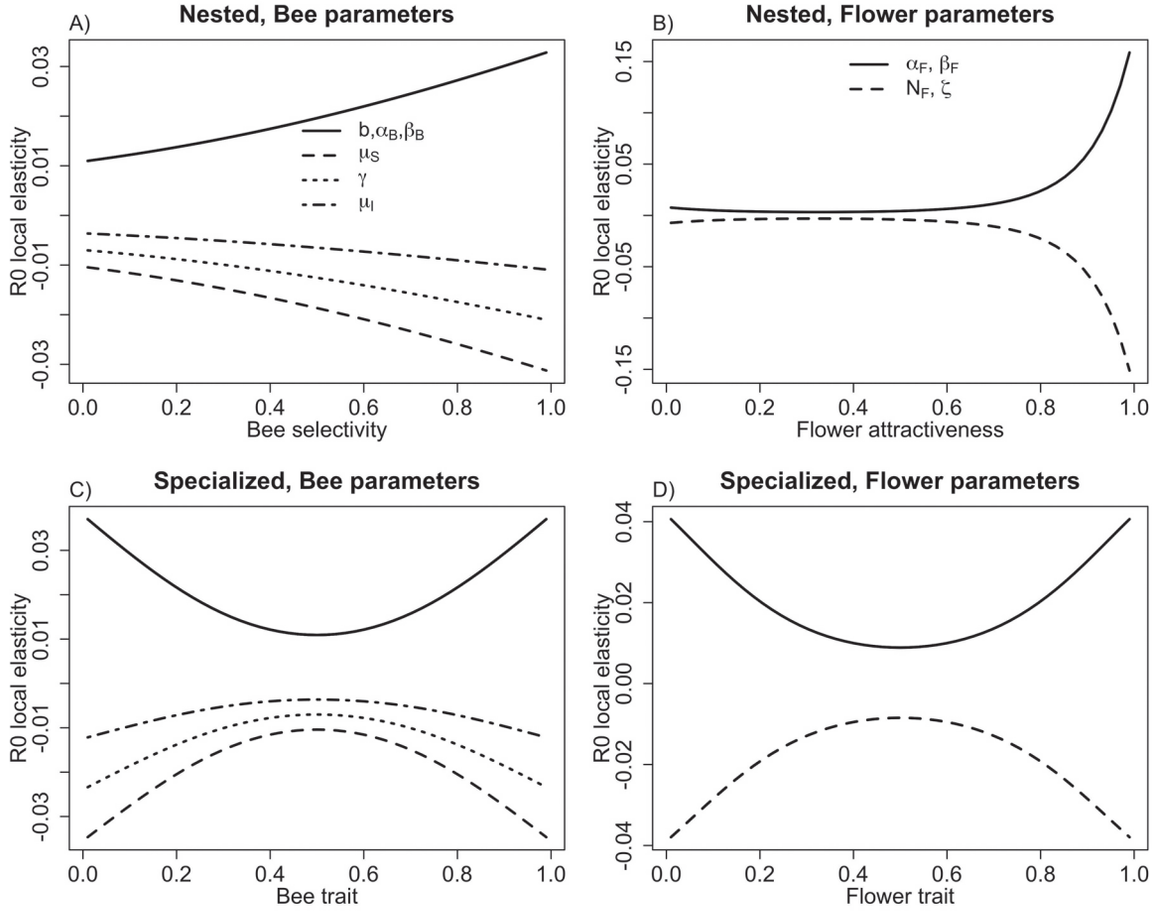

Figure 4: Local elasticity analysis of R_0 with nonuniform trait distribution in flowers (flower abundance $N_F(y)$ proportional to the curve in fig. S6 in the online appendix). *A*, *B*, Bee- and flower-specific parameters in the nested network model. *C*, *D*, Bee- and flower-specific parameters in the specialized network model. Parameters in *C* and *D* are the same as in *A* and *B*, respectively. This figure was produced by R0_local_elasticity_NF_NB.R and scripts that it sources (computer scripts deposited in the Dryad Digital Repository: https://dx.doi.org/10.5061/dryad.730n045; Truitt et al. 2019).

traits are less common than moderate traits, as shown in fig. S6).

When extreme flower traits are rare, flowers with rarer traits are more important, as shown in figure 4. In the nestedness case, the magnitude of the impact of rare, attractive flowers is greater than that of rare, unattractive flowers. In the specialization model, both of these magnitudes are equivalent. Similarly, in the specialization model, bees that visit rare flowers are more important than bees that visit common flowers. In the nestedness model, bees that visit attractive, rare flowers are even more important than bees that visit unattractive, rare flowers.

When extreme bee traits are rare, bees with common traits are more important, as shown in figure 5. Similarly, flowers that interact with common bee classes are also more important in the specialization model.

For both models and for nonuniform trait distributions in bees and flowers, R_0 local elasticity trends are preserved in the local elasticity analysis of steady-state pathogen prevalence (figs. S9, S10). All parameters have the same qualitative relationship between elasticity and trait value and the same direction of effect on R_0, but the magnitudes differ among the analyses.

The sensitivity results for nonuniform trait distributions reflect the change in disease prevalence across the network. With nonuniform flower trait distribution (fig. S7), in the nested network disease, prevalence is more concentrated in the most attractive flowers and specialized bees; in the specialization model, disease prevalence is concentrated in extreme-trait (rarer) flowers and the extreme-trait bees that visit them. With nonuniform bee-trait distribution (fig. S8), not much change is evident in the nested network, but in the specializa-

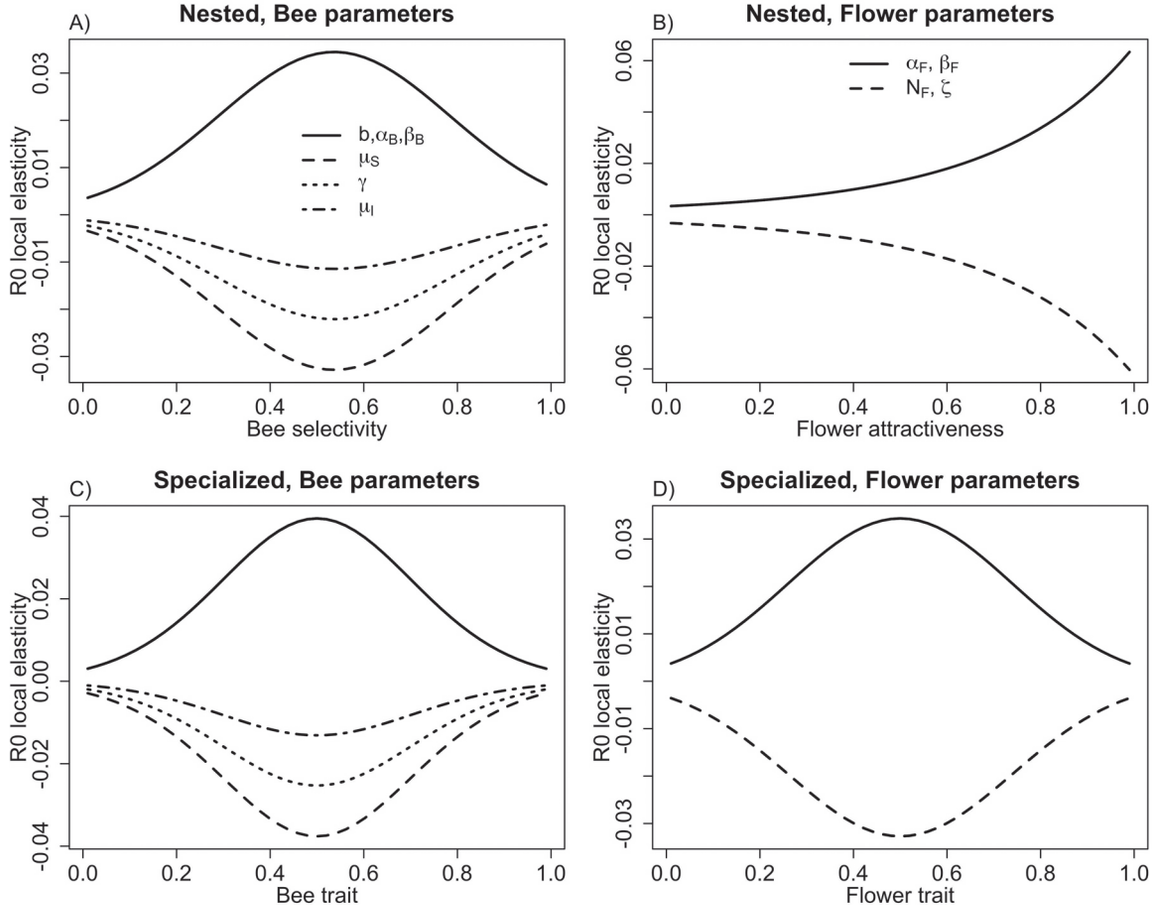

Figure 5: Local elasticity analysis of R_0 with nonuniform trait distribution in bees ($b(x)$ proportional to the curve in fig. S6 in the online appendix). *A*, *B*, Bee- and flower-specific parameters in the nested network model. *C*, *D*, Bee- and flower-specific parameters in the specialized network model. Parameters in *C* and *D* are the same as in *A* and *B*, respectively. This figure was produced by R0_local_elasticity_NF_NB.R and scripts that it sources (computer scripts deposited in the Dryad Digital Repository: https://dx.doi.org/10.5061/dryad.730n045; Truitt et al. 2019).

tion model, disease is now concentrated in intermediate-trait bees and in the intermediate-trait flowers that they interact with most.

Discussion

In this article, we proposed and studied a trait-based model of disease transmission in multihost plant-pollinator networks. While we applied our model to pollinators and pathogens, its framework is general enough that it can be applied to species interactions in any community. Thus, the goal of our model is not only to advance a trait-based approach for understanding disease transmission among pollinators but more generally for understanding multispecies communities. While promoting this approach, we do not deny that species identity matters and that it may be paramount in some cases. Instead, we are proposing that when species interactions are driven by functional traits, a trait-distribution model may be a much simpler approach to modeling the system (e.g., we used one parameter to describe a contact network driven by trait matching vs. hundreds to describe every pairwise interaction). Thus, a trait-based approach affords the model more predictive power and makes it easier to identify general properties of transmission in species interaction networks.

Empirical data on bees, pathogens, and flowers were gathered and used to parameterize plant-pollinator networks. We found that in the single-class model, the disease reproductive number has a quadratic relationship with pollinator contact rate (eq. [4]), analogous to the vector biting rate in models for vectored diseases. This finding is mirrored in the trait-based model, where the reproductive number is proportional to the dominant eigenvalue of $\mathbf{H}^{\mathrm{T}}\mathbf{H}$, where $\mathbf{H}$ is the operator with kernel $h(y, x)$ (eq. [12]). With uniform trait distributions, R_0 and disease prevalence were most sen-

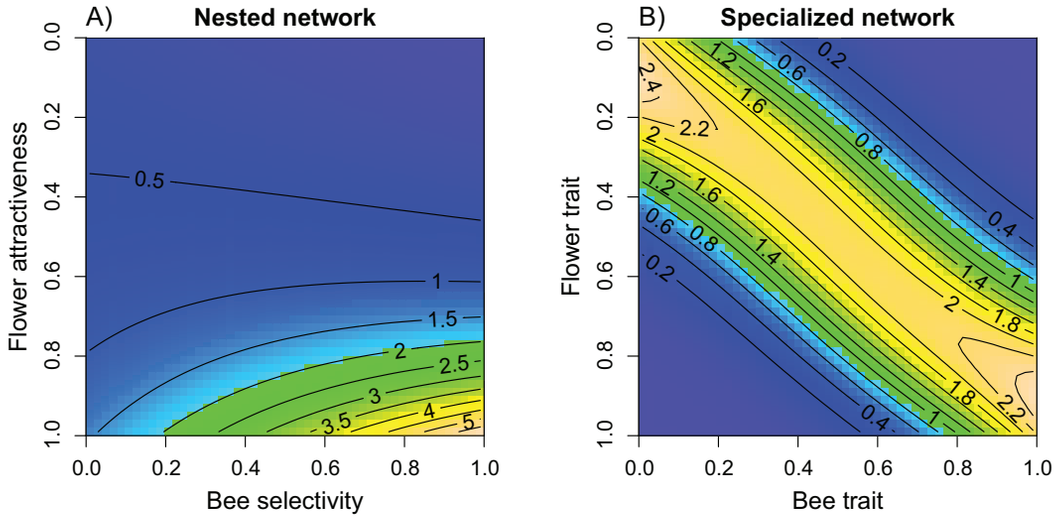

Figure 6: Local elasticity of R_0 with respect to pairwise transmission rates between bees and flowers of different classes at the default parameter values with uniform trait distributions. *A*, Nested network model with $n = 3$. *B*, Specialized network model with $\sigma = 10$. Because the unperturbed transmission matrix is symmetric in this case, elasticity for bee class x to flower class y transmission is the same as that for flower class y to bee class x transmission. Plotted values are scaled to represent elasticities in the continuous trait model (i.e., the integral of each elasticity surface is 1, corresponding to the fact that increasing all α values—or all β values—by a factor $1 + \varepsilon$ increases R_0 by the same factor). This figure was produced by ContactElasticityImages.R (computer scripts deposited in the Dryad Digital Repository: https://dx.doi.org/10.5061/dryad.730n045; Truitt et al. 2019), using the elasticity formulas derived in section S.3 of the online appendix.

sitive to selective bees and attractive flowers in the nested network model and to bees and flowers with intermediate trait values in the specialization model. Nonuniform trait distributions increased the importance of bees with more common trait values and of flowers with less common trait values. Our results regarding nestedness and specialization are likely generalizable because these attributes are extremely common in species interaction networks (e.g., Bascompte et al. 2003; Cantor et al. 2017). Indeed, there is some evidence that nestedness and specialization may arise as unavoidable spandrels in any community of interacting species (Maynard et al. 2018; Valverde et al. 2018).

A commonality across all analyses is that disease persistence and prevalence are most sensitive to areas of concentrated visitation in the network. Specifically, disease spread is sensitive to flower classes that are visited disproportionately often relative to their abundance and to the bee classes that collectively most often visit those flowers. In section 3.8, these importance measures based strictly on visitation rates are defined precisely and are shown to align closely with the results of elasticity analysis. These areas act as disease hot spots, the equivalent of a watering hole in trait space, where disease is prevalent and frequently transmitted. These findings are consistent with the empirical data from multihost systems where pronounced among-individual heterogeneity in transmission is often observed (Paull et al. 2012; Johnson et al. 2015*a*, 2015*b*). For example, among six grass species exposed to barley yellow dwarf virus, plants with high leaf nitrogen and high metabolic rates had higher susceptibility and larger vector populations, likely because their leaf traits offered more resources for vector and pathogen growth (Cronin et al. 2010). Similarly, species with highly social behavior can be at increased risk of contracting pathogens due to higher contact rates (Altizer et al. 2003). Furthermore, traits of the transmission environment have also been shown to be important. For example, across 120 vertebrate species in China that are competent hosts of *Schistosomiasis japonica*, in marshlands, bovids were the main source of transmission, whereas in hilly areas, rodents were the most important pathogen reservoirs (Rudge et al. 2013). Such examples highlight how host and reservoir traits can shape species interactions and transmission potential, similar to the results from our trait-based model.

We found that the value of R_0 was substantially decreased by increasing the population size of the flowers that were visited most often relative to their abundance. For example, R_0 decreased when the most attractive flowers increased in a nested network with uniform trait distributions. Additionally, R_0 was decreased by flowers that are attractive and rare in a nested network with nonuniform trait distributions and by flowers with intermediate traits in a specialized network with uniform trait distributions or with a high abundance of intermediate bee classes. While this initially seems counterintuitive, it is a dilution effect resulting from our assumption that increased flower abundance does not change the total number of visits a bee makes to all flowers com-

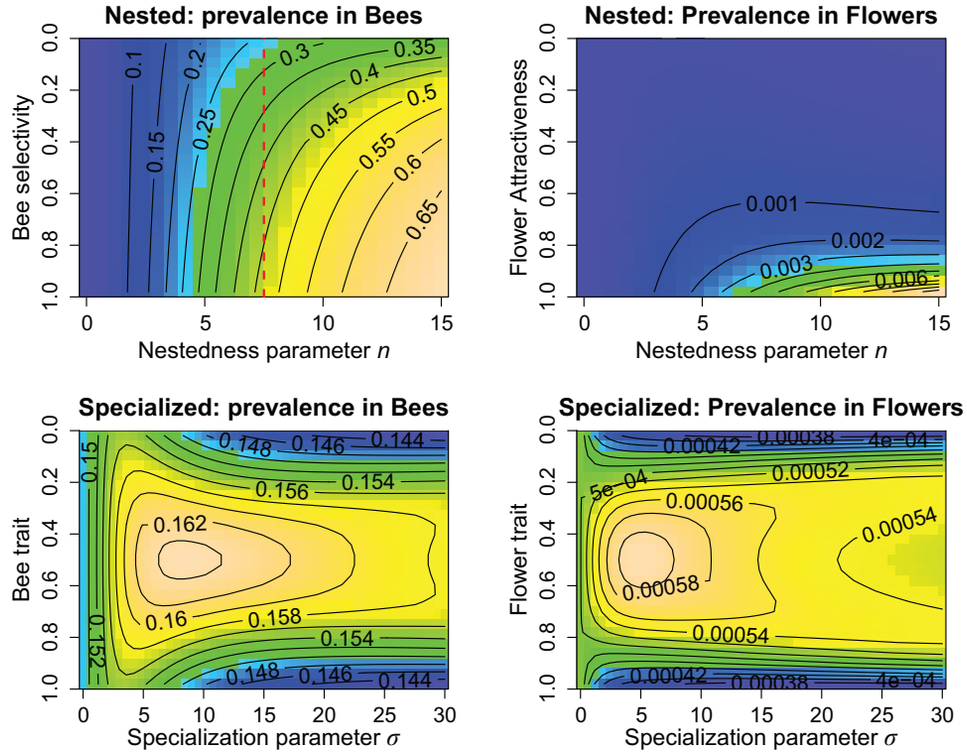

Figure 7: Image and contour plots of steady-state disease prevalence (proportion of infected individuals). In each panel, a vertical slice (such as the dashed red line, *top left*) represents disease prevalence as a function of bee or flower trait for a given value of the nestedness parameter n or specialization parameter σ. This figure was produced by SteadyStateImages.R (computer scripts deposited in the Dryad Digital Repository: https://dx.doi.org/10.5061/dryad.730n045; Truitt et al. 2019).

bined. Therefore, an increase in the popular flower population size decreases the likelihood that a bee comes in contact with any one single infected flower, thus potentially reducing pathogen spread. Such dilution effects are common in communities where species vary in reservoir competence, though the specific mechanisms underlying changes in disease prevalence and spread often are not known in empirical systems (Ostfeld and Keesing 2012).

Several aspects of our model could be improved and extended. First, for simplicity, our model assumed that plants and pollinators were each characterized by a single trait, but pollinators typically respond to multiple traits when choosing which flowers to visit. Flower morphology, scent, and even electrical field are important filters of visitation by bees and other pollinators (Raguso 2008; Ollerton et al. 2009; Clarke et al. 2013). Little is known regarding how pollinators integrate multiple traits, although such trait integration can influence flower choice (Chittka and Raine 2006) and might play an underappreciated role in structuring plant-pollinator networks (Junker et al. 2013). Coupled heterogeneities in multiple host, pathogen, or vector traits can have important impacts generally in host-pathogen systems (Vazquez-Prokopec et al. 2016). In our framework, transmission mediated by multiple traits could increase the importance of hot spots in trait space where multiple traits are all just right for the pathogen to establish, persist, and transmit across the network. The presence and nature of between-trait correlations could then be important factors in disease persistence and prevalence. Experiments investigating which particular traits lead to specialization on particular flowers and which traits characterize flower attractiveness in general could increase realism of the model. For example, a recent experiment found that manipulation of one floral trait (flower shape) greatly impacted plant-pollinator network structure (Urban-Mead 2017), which could impact patterns of disease transmission. Second, in addition to considering multiple traits, the model contains eight additional parameters (mortality, recovery, etc.) that each could be impacted by traits. Finally, our model does not consider direct host-to-host transmission, but such transmission occurs in social bees (e.g., Naug 2008), so combining intracolony dynamics with the plant-pollinator network will be necessary to account for patterns analogous to clustering in networks (e.g., Watts and Strogatz 1998; Eubank et al. 2004).

In conclusion, we introduced a new trait-based approach for predicting disease transmission in species-rich pollina-

tion networks that can also be applied more generally to any community of interacting organisms. Our model suggests that, all else being equal, greater nestedness and specialization both generally promote disease spread within a network through the creation of disease hot spots in trait space. Furthermore, these results suggest possible ways of limiting pollinator pathogens by targeted wildflower plantings that restructure the network. For example, maximizing forage for pollinators is typically the sole consideration when land managers design pollinator-friendly wildflower strips on public lands or near agricultural settings (Blaauw and Isaacs 2014; Landis 2017; Williams and Lonsdorf 2018). However, an additional consideration could be to plant floral mixtures containing species with traits that minimize disease transmission. By focusing on traits rather than species identities, recommendations could be general and therefore not require specific knowledge of every plant in every local environment. Such predictions clearly need to be tested empirically since any change could have multiple effects, but the potential benefits are clear. Because global pollinator declines are caused in part by pathogens, increased understanding of the factors governing pathogen transmission in plant-pollinator networks is important for improving pollinator health.

Acknowledgments

We thank members of the Ellner and McArt lab groups, Chris Myers, and our anonymous reviewers for helpful comments on the manuscript. Research reported in this publication was supported by the National Institute of General Medical Sciences of the National Institutes of Health (NIH; award R01GM122062). The content is solely the responsibility of the authors and does not necessarily represent the official views of the NIH.

Statement of authorship: S.P.E., S.H.M., and L.L.T. conceived the study. L.L.T. and S.H.M. provided parameters and justifications. L.L.T., S.P.E., and A.H.V. conducted simulations and mathematical analyses. L.L.T. wrote the original manuscript, which was revised jointly by all coauthors, and wrote portions of the appendixes; and S.P.E. and A.H.V. wrote portions of the appendixes.

APPENDIX

Additional Technical Information

Further Explanations of Parameter Estimates

N_F: We sampled five old fields in 2015 using modified-Whittaker sample plots. In each plot, we collected presence/absence data for each species in the full plot and larger subplots and recorded cover estimates for each plant species in 10 0.5×0.5-m quadrats. Because N_F is linked to bee-flower interactions in our model, our estimate is a combination of flower and inflorescence abundance depending on the plant species. For example, flowers from some species are too small for bees to interact with individually but instead are organized on an inflorescence that bees interact with as a group (e.g., *Solidago juncea*). Flowers from other species are large enough for bees to interact with individually (e.g., *Penstemon digitalis*). Thus, for each of the 53 plant species surveyed, we chose whether the flower or inflorescence was the most appropriate unit of measurement. To calculate flower/inflorescence density on a given day across the growing season, we first recorded the flower/inflorescence density for each species at peak bloom in a minimum of five 0.5×0.5-m quadrats. Next, we modeled the floral density of each species according to a normal distribution across the entire bloom period, with a maximum set at the peak bloom density. Bloom period data were based on local phenology data collected in the flora of the Cayuga Lake Basin, New York (Wiegand and Eames 1926).

b: This estimate gives $b \approx 0.032 \times (190–380) = (6.1–12.3)$.

μ_S: Winter honeybees are known to live longer than 7 weeks but are not included here because they are not actively foraging (and potentially transmitting pathogens at flowers) during the winter.

μ_I: The estimate implies $1/\mu_I = 0.63/\mu_S$; hence, $\mu_I = (1/0.63)\mu_S \approx 1.6\mu_S$. Thus, the range and default for μ_I are 1.6 times those for μ_S.

Numerical Global Elasticity Analyses

We ran 500,000 trials for each global sensitivity analysis of model parameters. In each trial, values within the ranges specified in table 1 were generated for each parameter for all bee and flower classes using Latin hypercube sampling (R function randomLHS in the sensitivity package; Pujol et al. 2017). Contact matrices were formed as specified in equation (13) or (14) according to each class's H_b, with $n = 3$ for nestedness and $\sigma = 10$ for specialization. For each trial, R_0 or disease steady state was calculated using that trial's parameter values. Once all trials were completed, a linear model was fit to the rank of the R_0's or the disease steady state's as a function of the rank of the parameter values used. The main script file is R0_global_sensitivity.R.

To determine the effect of n and σ on R_0, 10,000 sets of model parameters were generated as described in the previous paragraph and paired with 10,000 randomly generated values of n (uniform on (0, 15)) or σ (uniform on (0, 30)). We then recalculated R_0 for n or σ increased by 0.1. The main script file is R0_and_Network_global.R.

Literature Cited

Adler, L. S., K. M. Michad, S. P. Ellner, S. H. McArt, P. C. Stevenson, and R. E. Irwin. 2018. Disease where you dine: plant species and floral traits associated with pathogen transmission in bumble bees. Ecology 99:2535–2545.

Aizen, M. A., M. Sabatino, and J. M. Tilianakis. 2012. Specialization and rarity predict nonrandom loss of interactions from mutualist networks. Science 335:1486–1489.

Allison, S. D. 2012. A trait-based approach for modeling microbial litter decomposition. Ecology Letters 15:1058–1070.

Altizer, S., C. L. Nunn, P. H. Thrall, J. L. Gittleman, J. Antonovics, A. A. Cunningham, A. P. Dobson, et al. 2003. Social organization and parasite risk in mammals: integrating theory and empirical studies. Annual Review of Ecology, Evolution, and Systematics 34:517–547.

Barrett, S. C. H., and L. D. Harder. 2007. Ecology and evolution of flowers. Oxford University Press, New York.

Bascompte, J., and P. Jordano. 2007. Plant-animal mutualistic networks: the architecture of biodiversity. Annual Review of Ecology, Evolution, and Systematics 38:567–593.

Bascompte, J., P. Jordano, C. J. Melian, and J. M. Olesen. 2003. The nested assembly of plant-animal mutualistic networks. Proceedings of the National Academy of Sciences of the USA 100:9383–9387.

Betts, M. G., A. S. Hadley, and W. J. Kress. 2015. Pollinator recognition by a keystone tropical plant. Proceedings of the National Academy of Sciences of the USA 112:3433–3438.

Blaauw, B. R., and R. Isaacs. 2014. Flower plantings increase wild bee abundance and the pollination services provided to a pollination-dependent crop. Journal of Applied Ecology 51:890–898.

Burkle, L. A., J. C. Marlin, and T. M. Knight. 2013. Plant-pollinator interactions over 120 years: loss of species, co-occurrence and function. Science 339:1611–1615.

Cameron, S. A., J. D. Lozier, J. P. Strange, J. B. Koch, N. Cordes, L. F. Solter, and T. L. Griswold. 2011. Patterns of widespread decline in North American bumble bees. Proceedings of the National Academy of Sciences of the USA 108:662–667.

Cantor, M., M. M. Pires, F. M. Marquitti, R. L. Raimundo, E. Sebastian-Gonzalez, P. P. Coltri, S. I. Perez, et al. 2017. Nestedness across biological scales. PLoS ONE 12:e0171691.

Chittka, L., and N. E. Raine. 2006. Recognition of flowers by pollinators. Current Opinion in Plant Biology 9:428–435.

Clarke, D., H. Whitney, G. Sutton, and D. Robert. 2013. Detection and learning of floral electrical fields by bumblebees. Science 340:66–69.

Cornman, R. S., D. R. Tarpy, Y. Chen, L. Jeffreys, D. Lopez, J. S. Pettis, D. vanEngelsdorp, and J. D. Evans. 2012. Pathogen webs in collapsing honey bee colonies. PLoS ONE 7:e43562.

Couvillon, M. J., F. C. Riddell-Pearce, C. Accleton, K. A. Fensome, S. K. L. Quah, E. L. Taylor, and F. L. W. Ratnieks. 2015. Honey bee foraging distance depends on month and forage type. Apidologie 46:61–70.

Cronin, J. P., M. E. Welsh, M. G. Dekkers, S. T. Abercrombie, and C. E. Mitchell. 2010. Host physiological phenotype explains pathogen reservoir potential. Ecology Letters 13:1221–1232.

Diekmann, O., J. A. Heesterbeek, and M. G. Roberts. 2009. The construction of next-generation matrices for compartmental epidemic models. Journal of the Royal Society Interface 47:873–885.

Dobson, A. 2004. Population dynamics of pathogens with multiple host species. American Naturalist 164(suppl.):S64–S78.

Ellner, S. P., D. Z. Childs, and M. Rees. 2016. Data-driven modeling of structured populations: a practical guide to the integral projection model. Springer, New York.

Eubank, S., H. Guclu, V. S. Anil Kumar, M. V. Marathe, A. Srinivasan, Z. Toroczkai, and N. Wang. 2004. Modelling disease outbreaks in realistic urban social networks. Nature 429:180–184.

Evans, J. D., K. Aronstein, Y. P. Chen, C. Hetru, J.-L. Imler, H. Jiang, M. Kanost, G. J. Thompson, Z. Zou, and D. Hultmark. 2006. Immune pathways and defence mechanisms in honey bees *Apis mellifera*. Insect Molecular Biology 15:645–656.

Evison, S. E. F., K. E. Roberts, L. Laurenson, S. Pietravalle, J. Hui, J. C. Biesmeijer, J. E. Smith, G. Budge, and W. O. H. Hughes. 2012. Pervasiveness of parasites in pollinators. PLoS ONE 7:e30641.

Figueroa, L. L., M. Blinder, C. Grincavitch, A. Jelinek, E. Mann, L. Merva, L. Metz, A. Zhao, R. E. Irwin, S. H. McArt, and L. S. Adler. Forthcoming *a*. Bee pathogen transmission dynamics: deposition, persistence and acquisition on flowers. Proceedings of the Royal Society of London B.

Figueroa, L. L., H. Grab, P. Graystock, C. R. Myers, Q. S. McFrederick, and S. H. McArt. Forthcoming *b*. Landscape and interaction network structure drive pathogen prevalence in bee communities. Science.

Furst, M. A., D. P. McMahon, J. L. Osborne, R. J. Paxton, and M. J. F. Brown. 2014. Disease associations between honeybees and bumblebees as a threat to wild pollinators. Nature 506:364–366.

Gamboa, V., J. Ravoet, M. Brunain, G. Smagghe, I. Meeus, J. Figueroa, D. Riano, and D. C. de Graaf. 2015. Bee pathogens found in *Bombus atratus* from Colombia: a case study. Journal of Invertebrate Pathology 129:36–39.

Goulson, D. 2009. Bumblebees: behaviour, ecology, and conservation. Oxford University Press, New York.

Goulson, D., E. Nicholls, C. Botias, and E. L. Rotheray. 2015. Bee declines driven by combined stress from parasites, pesticides, and lack of flowers. Science 347:1435–1439.

Graystock, P., K. Yates, B. Darvill, D. Goulson, and W. O. H. Hughes. 2013*a*. Emerging dangers: deadly effects of an emergent parasite in a new pollinator host. Journal of Invertebrate Pathology 114:114–119.

Graystock, P., K. Yates, S. E. F. Evison, B. Darvill, D. Goulson, and W. O. H. Hughes. 2013*b*. The Trojan hives: pollinator pathogens, imported and distributed in bumblebee colonies. Journal of Applied Ecology 50:1207–1215.

Green, J. L., B. J. M. Bohannan, and R. J. Whitaker. 2008. Microbial biogeography: from taxonomy to traits. Science 320:1039–1043.

Griffiths, G. W. 2016. Numerical analysis using R: solutions to ODEs and PDEs. Cambridge University Press, Cambridge.

Han, B. A., J. P. Schmidt, S. E. Bowden, and J. M. Drake. 2015. Rodent reservoirs of future zoonotic diseases. Proceedings of the National Academy of Sciences of the USA 112:7039–7044.

Harder, L. D. 1983. Flower handling efficiency of bumble bees: morphological aspects of probing time. Oecologica 57:274–280.

Hawley, D. M., and S. M. Altizer. 2011. Disease ecology meets ecological immunology: understanding the links between organismal immunity and infection dynamics in natural populations. Functional Ecology 25:48–60.

Hillebrand, H., and B. Matthiessen. 2009. Biodiversity in a complex world: consolidation and progress in functional biodiversity research. Ecology Letters 12:1405–1419.

Hudson, P. J., S. E. Perkins, and I. M. Cattadori. 2008. The emergence of wildlife disease and the application of ecology. Pages 347–376 *in*

R. S. Ostfeld, F. Keesing, and V. T. Eviner, eds. Infectious disease ecology: effects of ecosystems on disease and of disease on ecosystems. Princeton University Press, Princeton, NJ.

Johnson, P. T. J., J. C. De Roode, and A. Fenton. 2015*a*. Why infectious disease research needs community ecology. Science 349:1069–1073.

Johnson, P. T. J., R. S. Ostfeld, and F. Keesing. 2015*b*. Frontiers in research on biodiversity and disease. Ecology Letters 18:1119–1133.

Junker, R. R., N. Bluthgen, T. Brehm, J. Binkenstein, J. Paulus, H. M. Schaefer, and M. Stang. 2013. Specialization on traits as basis for the niche-breadth of flower visitors and as structuring mechanism of ecological networks. Functional Ecology 27:329–341.

Kaya, H. K. 1977. Survival of spores of *Vairimorpha* (=*Nosema*) *necatrix* (Microsporida: Nosematidae) exposed to sunlight, ultraviolet radiation, and high temperature. Journal of Invertebrate Pathology 30:192–198.

Keeling, M. J., and P. Rohani. 2008. Modeling infectious diseases in humans and animals. Princeton University Press, Princeton, NJ.

Koch, H., M. J. F. Brown, and P. C. Stevenson. 2017. The role of disease in bee foraging ecology. Current Opinion in Insect Science 21:60–67.

Landis, D. A. 2017. Designing agricultural landscapes for biodiversity-based ecosystem services. Basic and Applied Ecology 18:1–12.

Lever, J. J., E. H. van Nes, M. Scheffer, and J. Bascompte. 2014. The sudden collapse of pollinator communities. Ecology Letters 17:350–359.

Li, J., D. Blakeley, and R. J. Smith. 2011. The failure of R_0. Computational and Mathematical Methods in Medicine 2011:527610.

Lloyd-Smith, J. O., M. Poss, and B. T. Grenfell. 2008. HIV-1/parasite co-infection and the emergence of new parasite strains. Parasitology 135:795–806.

Luis, A. D., T. J. O'Shea, D. T. S. Hayman, J. L. N. Wood, A. A. Cunningham, A. T. Gilbert, J. N. Mills, and C. T. Webb. 2015. Network analysis of host-virus communities in bats and rodents reveals determinants of cross-species transmission. Ecology Letters 18:1153–1162.

MacDonald, G. 1952. The analysis of equilibrium in malaria. Tropical Diseases Bulletin 49:813–829.

Mandelik, Y., R. Winfree, T. Neeson, and C. Kremen. 2012. Complementary habitat use by wild bees in agro-natural landscapes. Ecological Applications 22:1535–1546.

Maynard, D. S., C. A. Servan, and S. Allesina. 2018. Network spandrels reflect ecological assembly. Ecology Letters 21:324–334.

McArt, S. H., H. Koch, R. E. Irwin, and L. S. Adler. 2014. Arranging the bouquet of disease: floral traits and the transmission of plant and animal pathogens. Ecology Letters 17:624–636.

McArt, S. H., C. Urbanowicz, S. McCoshum, R. E. Irwin, and L. S. Adler. 2017. Landscape predictors of pathogen prevalence and range contractions in US bumblebees. Proceedings of the Royal Society B 284:20172181.

McGill, B. J., B. J. Enquist, E. Weiher, and M. Westoby. 2006. Rebuilding community ecology from functional traits. Trends in Ecology and Evolution 21:178–185.

McMahon, D. P., M. A. Furst, J. Caspar, P. Theodorou, M. J. F. Brown, and R. J. Paxton. 2015. A sting in the spit: widespread cross-infection of multiple RNA viruses across wild and managed bees. Journal of Animal Ecology 84:615–624.

McMahon, D. P., M. E. Natsopoulou, V. Doublet, M. A. Furst, S. Weging, M. J. F. Brown, A. Gogo-Doring, and R. J. Paxton. 2016. Elevated virulence of an emerging viral genotype as a driver of honeybee loss. Proceedings of the Royal Society B 283:20160811.

Memmott, J., N. M. Waser, and M. V. Price. 2004. Tolerance of pollination networks to species extinctions. Proceedings of the Royal Society B 1557:2605–2611.

Merikanto, I., J. Laakso, and V. Kaitala. 2012. Outside-host growth of pathogens attenuates epidemiological outbreaks. PLoS ONE 7:e50158.

Michener, C. D. 1974. The bees of the world. Johns Hopkins University Press, Baltimore.

———. 2007. The social behavior of the bees. Harvard University Press, Cambridge, MA.

Miller-Struttmann, N. E., J. C. Geib, J. D. Franklin, P. G. Kevan, R. M. Holdo, D. Ebert-May, and C. Galen. 2015. Functional mismatch in a bumble bee pollination mutualism under climate change. Science 349:1541–1544.

Naug, D. 2008. Structure of the social network and its influence on transmission dynamics in a honeybee colony. Behavioral Ecology and Sociobiology 62:1719–1725.

Ollerton, J., R. Alarcon, N. M. Waser, M. V. Price, S. Watts, L. Cranmer, A. Hingston, C. I. Peter, and J. Rotenberry. 2009. A global test of the pollination syndrome hypothesis. Annals of Botany 103:1471–1480.

Ostfeld, R. S., and F. Keesing. 2012. Effects of host diversity on infectious disease. Annual Review of Ecology, Evolution, and Systematics 43:157–182.

Otterstatter, M. C., and J. D. Thomson. 2007. Contact networks and transmission of an intestinal pathogen in bumble bee (*Bombus impatiens*) colonies. Oecologia 154:411–421.

Paull, S. H., S. Song, K. M. McClure, L. C. Sackett, A. M. Kilpatrick, and P. T. J. Johnson. 2012. From superspreaders to disease hotspots: linking transmission across hosts and space. Frontiers in Ecology and the Environment 10:75–82.

Paxton, R., J. Klee, S. Korpela, and I. Fries. 2007. *Nosema ceranae* has infected *Apis mellifera* in Europe since at least 1998 and may be more virulent than *Nosema apis*. Apidologie 38:558–565.

Perkins, S. E., I. M. Cattadori, V. Tagliapietra, A. P. Rizzoli, and P. J. Hudson. 2003. Empirical evidence for key hosts in persistence of a tick-borne disease. International Journal for Parasitology 33:909–917.

Pujol, G., B. Iooss, and A. Janon. 2017. Sensitivity: global sensitivity analysis of model outputs. R package version 1.14.0. https://CRAN.R-project.org/package=sensitivity.

Raguso, R. A. 2008. Wake up and smell the roses: the ecology and evolution of floral scent. Annual Review of Ecology, Evolution, and Systematics 39:549–569.

Ravoet, J., L. De Smet, I. Meeus, G. Smagghe, T. Wenseleers, and D. C. de Graaf. 2014. Widespread occurrence of honey bee pathogens in solitary bees. Journal of Invertebrate Pathology 122:55–58.

Retschnig, G., G. R. Williams, M. M. Mehmann, O. Yanez, J. R. Miranda, and P. Neumann. 2014. Sex-specific differences in pathogen susceptibility in honey bees (*Apis mellifera*). PLoS ONE 9:e85261.

Rudge, J. W., J. P. Webster, D. B. Lu, T. P. Wang, G. R. Fang, and M. G. Basanez. 2013. Identifying host species driving transmission of schistosomiasis japonica, a multihost parasite system, in China. Proceedings of the National Academy of Sciences of the USA 110:11457–11462.

Rudolf, V. H., and J. Antonovics. 2005. Species coexistence and pathogens with frequency-dependent transmission. American Naturalist 166:112–118.

Ruiz-Gonzalez, M. X., J. Bryden, Y. Moret, C. Reber-Funk, P. Schmid-Hempel, and M. J. F. Brown. 2012. Dynamic transmission, host quality, and population structure in a multihost parasite of bumblebees. Evolution 66:3053–3066.

Salathe, M., M. Kazandjieva, J. W. Lee, P. Levis, M. W. Feldman, and J. H. Jones. 2010. A high-resolution human contact network for infectious disease transmission. Proceedings of the National Academy of Sciences of the USA 107:22020–22025.

Schmidt, K. A., and R. S. Ostfeld. 2001. Biodiversity and the dilution effect in disease ecology. Ecology 82:609–619.

Smith, D. L., K. E. Battle, S. I. Hay, C. M. Barker, T. W. Scott, and F. E. Mckenzie. 2012. Ross, Macdonald, and a theory for the dynamics and control of mosquito-transmitted pathogens. PLoS Pathogens 8:e1002588.

Soetaert, K., T. Petzoldt, and R. W. Setzer. 2010. Solving differential equations in R: package deSolve. Journal of Statistical Software 33:1–25. doi:10.18637/jss.v033.i09.

Stohlgren, T. J. 2007. Measuring plant diversity. Oxford University Press, New York.

Strauss, A. T., A. M. Bowling, M. A. Duffy, C. E. Cáceres, and S. R. Hall. 2018. Linking host traits, interactions with competitors and disease: mechanistic foundations for disease dilution. Functional Ecology 32:1271–1279.

Streicker, D. G., A. Fenton, and A. B. Pedersen. 2013. Differential sources of host species heterogeneity influence the transmission and control of multihost parasites. Ecology Letters 16:975–984.

Stutz, W. E., O. L. Lau, and D. I. Bolnick. 2014. Contrasting patterns of phenotype-dependent parasitism within and among populations of threespine stickleback. American Naturalist 183:810–825.

Truitt, L. L., S. H. McArt, A. H. Vaughn, and S. P. Ellner. 2019. Data from: Trait-based modeling of multi-host pathogen transmission: plant-pollinator networks. American Naturalist, Dryad Digital Repository, http://dx.doi.org/10.5061/dryad.730n045.

Urban-Mead, K. R. 2017. Predictability of bee community composition after floral removals differs by floral trait group. Biology Letters 13:20170515.

Valverde, S., J. Pinero, B. Corominas-Murta, J. Montoya, L. Joppa, and R. Sole. 2018. The architecture of mutualistic networks as an evolutionary spandrel. Nature Ecology and Evolution 2:94–99.

Vazquez-Prokopec, G. M., T. A. Perkins, L. A. Waller, A. L. Lloyd, R. C. Reiner Jr., T. W. Scott, and U. Kitron. 2016. Coupled heterogeneities and their impact on parasite transmission and control. Trends in Parasitology 32:356–367.

Visscher, P. K., and T. D. Seeley. 1982. Foraging strategy of honeybee colonies in a temperate deciduous forest. Ecology 63:1790–1801.

Waddington, K. D., T. J. Herbert, P. K. Visscher, and M. R. Richter. 1994. Comparisons of forager distributions from matched honey bee colonies in suburban environments. Behavioral Ecology and Sociobiology 35:423–429.

Watts, D. J., and S. H. Strogatz. 1998. Collective dynamics of "small-world" networks. Nature 393:440–442.

Webb, C. T., J. A. Hoeting, G. M. Ames, M. I. Pyne, and N. L. Poff. 2010. A structured and dynamic framework to advance traits-based theory and prediction in ecology. Ecology Letters 13:267–283.

White, L. A., J. D. Forester, and M. E. Craft. 2017. Using contact networks to explore mechanisms of parasite transmission in wildlife. Biological Reviews 92:389–409.

Wiegand, K., and A. Eames. 1926. The flora of the Cayuga Lake basin, New York. Cornell University, Ithaca, NY.

Williams, N. M., and E. V. Lonsdorf. 2018. Selecting cost-effective plant mixes to support pollinators. Biological Conservation 217:195–202.

Winston, M. L. 1987. Biology of the honey bee. Harvard University Press, Cambridge, MA.

Yang, H. M. 2014. The basic reproduction number obtained from Jacobian and next generation matrices: a case study of dengue transmission modeling. Biosystems 126:52–75.

Zurbuchen, A., C. Bachofen, A. Muller, S. Hein, and S. Dorn. 2010. Are landscape structures insurmountable barriers for foraging bees? a mark-recapture study with two solitary pollen specialist species. Apidologie 41:497–508.

Associate Editor: Nicole Mideo
Editor: Russell Bonduriansky